Cyclotron instabilities driven by temperature anisotropy in the solar wind

N. Noreen, P. H. Yoon, and S. Zaheer

Citation: Physics of Plasmas **24**, 102902 (2017); doi: 10.1063/1.4999339
View online: http://dx.doi.org/10.1063/1.4999339
View Table of Contents: http://aip.scitation.org/toc/php/24/10
Published by the American Institute of Physics

Cyclotron instabilities driven by temperature anisotropy in the solar wind

N. Noreen,[1,2] P. H. Yoon,[2,3,4,a)] and S. Zaheer[1]
[1]*Department of Physics, Forman Christian College, Lahore, Pakistan*
[2]*IPST, University of Maryland, College Park, Maryland 20742, USA*
[3]*School of Space Research, Kyung Hee University, Yongin, Gyeonggi-Do 446-701, South Korea*
[4]*Korea Astronomy and Space Science Institute, Daejeon 305-348, South Korea*

(Received 7 August 2017; accepted 27 September 2017; published online 12 October 2017)

Kinetic plasma instabilities are important for regulating the temperature anisotropies of electrons and ions in solar wind. For the low beta regime, it is known that electromagnetic ion/electron cyclotron instabilities are important, but in the literature these unstable modes are discussed under the assumption of parallel propagation. The present paper extends the analysis to two (or with cylindrical symmetry, three) dimensions. The analysis is further extended to include quasilinear description with the assumption of the bi-Maxwellian velocity distribution function. Such an analysis lays the foundation for an eventual study in which cyclotron instabilities as well as obliquely propagating unstable modes such as the mirror instability are simultaneously taken into account. The present paper first lays down the basis for such future efforts in which the two- or three dimensional linear and quasilinear theories of cyclotron instabilities in the low beta regime are formulated. *Published by AIP Publishing.* https://doi.org/10.1063/1.4999339

I. INTRODUCTION

Electromagnetic cyclotron instabilities driven by excessive perpendicular temperature associated with ions (protons) and electrons are operative in various space plasma environments including the magnetosheath region of the Earth and other magnetized planets, solar wind and interplanetary space, and near the Sun's coronal environment. Electromagnetic ion cyclotron or EMIC instability is operative near the proton cyclotron frequency, while Electromagnetic electron cyclotron or EMEC instability is a high frequency mode operative in the vicinity of the electron cyclotron frequency. For high beta conditions, where beta is the ratio of thermal to magnetic energy densities in plasma, the same free energy source also excites the electron/ion mirror mode, which is an aperiodic (or purely growing) instability. For low beta situations, it is well known that the mirror mode has a much weaker growth rate when compared with the cyclotron instabilities so that the instabilities operative near the cyclotron frequency are the dominant unstable modes.[1]

In the literature, these cyclotron instabilities are usually discussed with the assumption of the wave vector parallel to the ambient magnetic field, e.g., Ref. 2. Such an assumption is valid if the beta value is moderate. However, for low beta conditions the electron cyclotron instability (EMEC) can have maximum growth occurring in wave propagation directions that are oblique to the ambient magnetic field.[3,4] For protons (EMIC), this behavior of shifting to the oblique direction of maximum growth for low beta is not discussed in the literature, but the generalization of both cyclotron instabilities to include arbitrary angles of propagation is useful and sometimes necessary. This is because, the aperiodic mirror instabilities driven by either electron or proton temperature anisotropy may compete for the same available free energy so that in the nonlinear stage of the instability one must treat the cyclotron and mirror instabilities in the same footing. Such a coupled interaction of different unstable modes in the nonlinear stage is demonstrated in a recent paper by Ahmadi *et al.*,[5] where the authors employed the two-dimensional particle-in-cell simulation technique to study the nonlinear evolution of combined proton and electron mirror as well as cyclotron instabilities. Similar results were also obtained by Riquelme *et al.*[6] as well.

The purpose of the present paper is to set the stage, as it were, for an eventual analytical study of the competition between different unstable modes in order to affect the plasma dynamics. More precisely, the eventual goal is to undertake the study of quasilinear analysis in which, cyclotron and aperiodic instabilities are treated simultaneously. In the present paper, we first formulate the linear and quasilinear theory of cyclotron instabilities separately, with an arbitrary wave propagation direction. In the literature, the oblique EMEC instability for the low electron beta situation has been studied by the numerical Vlasov dispersion relation solver[3] combined with the particle-in-cell simulation approach.[4] In the present paper, we employ an analytical methodology, which closely resembles the formalism developed for the magnetoionic theory. The quasilinear theory of two-dimensional cyclotron instabilities within the formalism to be discussed in the present paper has not been discussed in the literature. To reiterate, we may combine the formalism of the present paper and a recently formulated analytical quasilinear theory of electron/proton mirror instability[7] in order to investigate the above-mentioned competition between different unstable modes within the context of the quasilinear theory.

The significance of the cyclotron and other temperature anisotropy-driven instabilities in the context of solar wind and heliospheric physics was already alluded to previously, but more specifically, their relevance is in the context of understanding the origin of measured temperature anisotropies

a)Electronic mail: yoonp@umd.edu

associated with various charged particles in the solar wind. According to the simple macroscopic adiabatic theory, the solar wind should exhibit large excessive parallel temperature anisotropy as a result of expansion and conservation of the first adiabatic invariant. However, observed solar wind instead features quasi-isotropic thermal distribution with the moderate anisotropic temperature ratio apparently limited between the upper and lower bounds corresponding to various marginal stability (or threshold) conditions for various temperature anisotropy-driven instabilities. These instabilities include the proton and electron cyclotron (EMIC/EMEC) as well as the mirror and firehose instabilities.[8–13] It is one of the outstanding problems in the contemporary space and astrophysics to incorporate the effects of plasma instabilities in the global model of the solar wind.[14–18] In any comprehensive model of solar wind, it is imperative that one allows multiple unstable modes to simultaneously interact with each other. For such a task, one must generally treat EMIC/EMEC instabilities in two- or three-dimensional configurations. Among theoretical approaches in the literature, Yoon and Seough[19] approached the combined effects of mirror and EMIC (or proton cyclotron) instabilities, but in their work the basic formalism is applicable to low frequency proton mirror and EMIC only. The present paper aims to make a preliminary contribution toward the goal of formulating linear and quasilinear theories of both EMIC and EMEC instabilities. We pay particular attention to the situation for which analytical treatment is feasible.

The structure of the present paper is as follows: in Sec. II, we formulate the analytical theory of two- or three-dimensional cyclotron instabilities. In Sec. II A, we consider the low frequency EMIC instability, while Sec. II B is devoted to high frequency EMEC instability. Section II also presents numerical examples, which include the marginal instability threshold curves in the temperature ratio *versus* parallel beta parameter space, and we compare the difference between treating the cyclotron instabilities exactly *versus* the approximate analytical method. Section III is devoted to the quasilinear theoretical formulation of EMIC and EMEC instabilities, and we also discuss sample numerical results thereof. Finally, Sec. IV summarizes the findings.

II. WEAKLY UNSTABLE EMIC AND EMEC INSTABILITIES

In the present analysis, we consider a magnetized plasma with the ambient magnetic field directed along the z axis. The wave vector is assumed to lie in the xz plane, without the loss of generality, with θ designating the angle between the $\mathbf{k}$ vector and ambient magnetic field vector $\mathbf{B}_0$. The plasma frequency defined with respect to ions (protons) and electrons is given by $\omega_{pi} = (4\pi n_0 e^2/m_i)^{1/2}$ and $\omega_{pe} = (4\pi n_0 e^2/m_e)^{1/2}$, respectively, where e is the unit electric charge, n_0 is the ambient density, and m_i and m_e are proton and electron rest masses, respectively. The cyclotron frequency for protons and electrons is defined by $\Omega_i = eB_0/m_i c$ and $\Omega_e = eB_0/m_e c$, respectively, where c is the speed of light *in vacuo*.

We are primarily interested in physical situations where either of the temperature ratios $T_{\perp i}/T_{\parallel i}$ and $T_{\perp e}/T_{\parallel e}$ are only slightly higher than unity while the parallel betas $\beta_{\parallel i}$ and $\beta_{\parallel e}$ are arbitrary, or where beta values are low while the temperature ratio may not necessarily be low. In other words, we are interested in situations where the instabilities have weak growth rates and the physical system is close to marginally unstable states. Here, betas for each species, defined with respect to the perpendicular and parallel temperatures, are given by $\beta_{\perp i} = 8\pi n_0 T_{\perp i}/B_0^2$, $\beta_{\parallel i} = 8\pi n_0 T_{\parallel i}/B_0^2$, $\beta_{\perp e} = 8\pi n_0 T_{\perp e}/B_0^2$, and $\beta_e = 8\pi n_0 T_{\parallel e}/B_0^2$, where n_0 is the ambient plasma density and B_0 is the ambient magnetic field intensity. We assume that the growth rate for the cyclotron instabilities is low so that the customary formulae for weakly unstable or weakly damped modes are applicable. In such cases, it is known that weak electromagnetic ion cyclotron (EMIC) or weak electromagnetic electron cyclotron (EMEC or whistler) instabilities are excited. In the literature, as noted in the Introduction, these unstable modes are treated with the assumption of parallel propagation ($\theta = 0$). However, we are presently interested in extending the customary theory to include the finite propagation angle, $\theta \neq 0$. For the arbitrary angle, the general dispersion relation becomes quite complex for either instabilities. This is why we seek to formulate the analytical theories in the present paper. Before we move on to the general formulation of EMIC and EMEC instabilities for the arbitrary angle of wave propagation within the framework of the analytical theory, let us ascertain the validity of the analytical approach within the assumption of parallel propagation for which, exact formalism is rigorously applicable. Thus, the limit of applicability of analytical formulae is first considered next with the assumption of parallel propagation. After we ascertain the conditions for the validity for parallel propagation, we will extrapolate the result to the arbitrary propagation angle.

A. Limits of applicability of the analytical approach: Parallel propagation

Since EMIC and EMEC instabilities are driven separately by either proton or electron temperature anisotropy, and they are operative over vastly different frequency and wave number domains, in what follows, we discuss the two instabilities separately.

In the case of parallel propagation, the left-hand circularly polarized EMIC mode dispersion relation under the assumption of bi-Maxwellian proton distribution is given by—see, e.g.,[20–22]

$$0 = \frac{c^2 k_\parallel^2}{\omega_{pi}^2} + \frac{\omega}{\Omega_i} - \left(\frac{T_{\perp i}}{T_{\parallel i}} - 1\right) - \left[\frac{T_{\perp i}}{T_{\parallel i}}\,\omega - \left(\frac{T_{\perp i}}{T_{\parallel i}} - 1\right)\Omega_i\right] \frac{1}{k_\parallel \alpha_{\parallel i}}\, Z\left(\frac{\omega - \Omega_i}{k_\parallel \alpha_{\parallel i}}\right), \quad (1)$$

where $\alpha_{\parallel i} = \sqrt{2T_{\parallel i}/m_i}$ is the parallel thermal speed of the Maxwellian proton distribution. Of course, the above dispersion relation given in terms of the transcendental plasma

dispersion function $Z(\zeta) = \pi^{-1/2}\int_{-\infty}^{\infty} dx\, e^{-x^2}(x-\zeta)$, $\mathrm{Im}(\zeta) > 0$, can be solved by numerical means. However, once we allow finite $k_\perp$, the above relatively simple form of the dispersion relation becomes rather complicated, which is why we seek the analytical method. We hereby first seek to check the validity and range of applicability of the approximate analytical approach, according to which, the real frequency $\omega_r = \mathrm{Re}(\omega)$ and the growth/damping rate $\gamma = \mathrm{Im}(\omega)$ are given by

$$\omega_r = \frac{\Omega_i}{2}\left(\sqrt{\kappa^4+4\kappa^2}-\kappa^2\right),$$
$$\gamma = -\frac{\pi^{1/2}\,(\Omega_i-\omega_r)}{(2\Omega_i-\omega_r)\omega_r}\left[\frac{T_{\perp i}}{T_{\|i}}\frac{\omega_r}{\Omega_i}-\left(\frac{T_{\perp i}}{T_{\|i}}-1\right)\right]\zeta\, e^{-\zeta^2}, \quad (2)$$
$$\kappa = \frac{ck_\|}{\omega_{pi}}, \quad \zeta = \frac{\Omega_i-\omega_r}{k_\|\alpha_{\|i}}.$$

In Fig. 1, we demonstrate the validity of the approximate approach by way of plotting maximum growth rates computed on the basis of exact *versus* analytical formulae, (1) and (2), respectively. The contours of the maximum growth rate $\gamma_{\max}/\Omega_i$ are shown in the parameter space $(\beta_{\|i}, T_{\perp i}/T_{\|i})$. The solid curves represent the exact solution, while the dashed curves belong to the analytical calculation. As one can see, for sufficiently low maximum growth rates, say for $\gamma_{\max}/\Omega_i = 10^{-3}$ or so, the two approaches yield qualitatively similar results, as the two contours lie close to each other. For $\gamma_{\max}/\Omega_i = 10^{-2}$, the discrepancy already becomes apparent. For even higher growth rates, it is apparent that the approximate analytical formula fails. We will thus make use of this result for parallel propagation as a guide in the more general case. The sample set of input parameters $(\beta_{\|i}, T_{\perp i}/T_{\|i}) = (0.1, 2.24)$, (1,1.52), and (6.3,1.15) are shown with dots. For such choices, the analytical approach is arguably applicable, since the maximum growth rate contours nearly overlap.

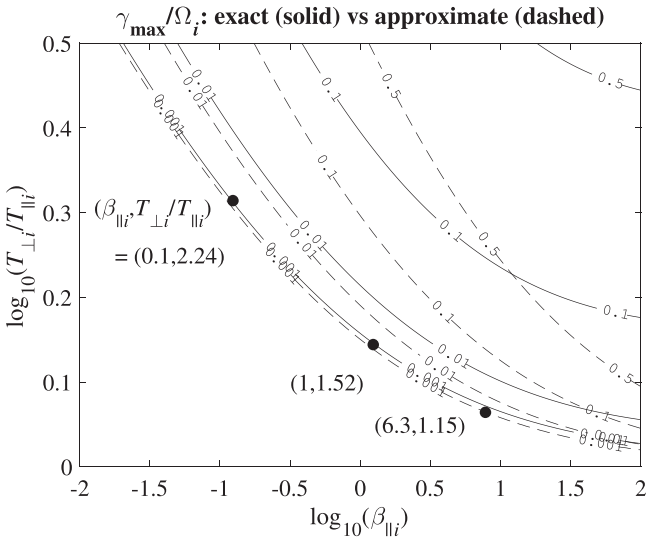

FIG. 1. Maximum growth rate of EMIC instability, $\gamma_{\max}/\Omega_i$ *versus* $\beta_{\|i}$ and $T_{\perp i}/T_{\|i}$, computed on the basis of exact dispersion relation (1), the contours of constant values of $\gamma_{\max}/\Omega_i$ plotted with solid curves, and computed on the basis of approximate analytical formula (2), the corresponding contours of which are shown with dashes. The dots represent sample sets of $\beta_{\|i}$ and $T_{\perp i}/T_{\|i}$ for which the analytical theory is valid.

These choices of parameters will be used in the subsequent calculation for arbitrary angles of wave propagation.

For the right-hand circularly polarized EMEC mode propagating parallel to the ambient magnetic field, the dispersion relation for the bi-Maxwellian electron distribution is given by[20]

$$0 = \frac{c^2k_\|^2}{\omega_{pe}^2} - \left(\frac{T_{\perp e}}{T_{\|e}}-1\right) - \left[\frac{T_{\perp e}}{T_{\|e}}\,\omega - \left(\frac{T_{\perp e}}{T_{\|e}}-1\right)\Omega_e\right]\frac{1}{k_\|\alpha_{\|e}}\,Z\left(\frac{\omega-\Omega_e}{k_\|\alpha_{\|e}}\right), \quad (3)$$

where $\alpha_{\|e} = \sqrt{2T_{\|e}/m_e}$ is the parallel thermal speed of the Maxwellian electron distribution. Under the approximate analytical approach, the real frequency $\omega_r = \mathrm{Re}(\omega)$ and the growth/damping rate $\gamma = \mathrm{Im}(\omega)$ are given by

$$\omega_r = \frac{\Omega_e\kappa^2}{1+\kappa^2},$$
$$\gamma = \frac{\pi^{1/2}\Omega_e^2}{(1+\kappa^2)^3 k_\|\alpha_{\|e}}\left(\frac{T_{\perp e}}{T_{\|e}}-1-\kappa^2\right)e^{-\zeta^2}, \quad (4)$$
$$\kappa = \frac{ck_\|}{\omega_{pe}}, \quad \zeta = \frac{\Omega_e}{(1+\kappa^2)k_\|\alpha_{\|e}}.$$

Figure 2 plots the exact maximum growth rate (solid contours) and approximate analytical formulae (dashed contours). As with Fig. 1, for sufficiently low maximum growth rates the two approaches yield qualitatively similar results. As with the case of EMIC, sample input parameters of $(\beta_{\|e}, T_{\perp e}/T_{\|e}) = (0.01, 4.5)$, (1,1.4125), and (5.6,1.12) are indicated. The subsequent calculation for arbitrary propagation angles will be based on these choices.

Figure 3 displays the exact growth rate computed on the basis of Eq. (1) *versus* approximate growth rate formula (2) for EMIC instability for the three cases indicated in Fig. 1.

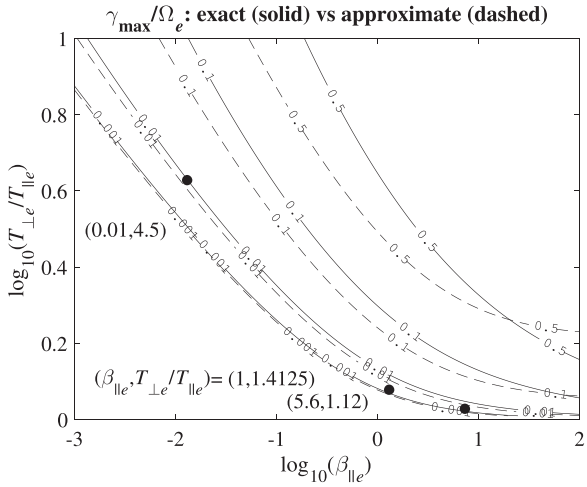

FIG. 2. Maximum growth rate of EMEC instability, $\gamma_{\max}/\Omega_e$ *versus* $\beta_{\|e}$ and $T_{\perp e}/T_{\|e}$, computed on the basis of exact dispersion relation (3), the contours of constant values of $\gamma_{\max}/\Omega_e$ plotted with solid curves, and computed on the basis of approximate analytical formula (4), the corresponding contours of which are shown with dashes. The dots represent sample values of $\beta_{\|e}$ and $T_{\perp e}/T_{\|e}$ for which the analytical theory is valid.

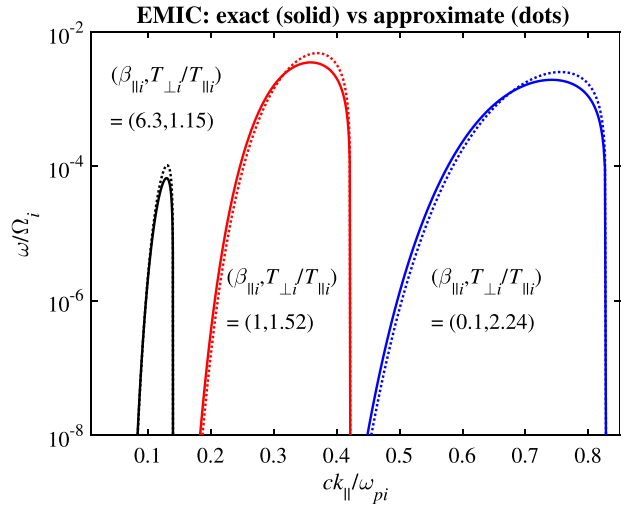

FIG. 3. Exact (solid lines) *versus* approximate (dotted lines) growth rates of EMIC instability, γ/Ω_i *versus* $ck_\|/\omega_{pi}$, for $(\beta_{\|i},T_{\perp i}/T_{\|i}) = (0.1, 2.24)$ (blue), $(\beta_{\|i},T_{\perp i}/T_{\|i}) = (1, 1.52)$ (red), and $(\beta_{\|i},T_{\perp i}/T_{\|i}) = (6.3, 1.15)$ (black).

Note how the two growth rates agree reasonably, albeit the approximate growth rate is somewhat higher in magnitude. The real frequencies computed either way also show excellent agreement, which we do not show.

In Fig. 4, we repeat the same analysis for EMEC, comparing the exact growth rate numerically computed from solving Eq. (3), *versus* the analytical approximation based upon Eq. (4). Again, the approaches produce comparable results. The real frequency associated with the whistler-EMEC mode shows excellent convergence between the exact *versus* analytical formulae, so we do not show the rather trivial comparisons.

On the basis of these findings for parallel propagation, we now extrapolate the analysis to include the finite perpendicular wave number. The analysis of arbitrary propagation angles will be formulated in Sec. II B, but the actual

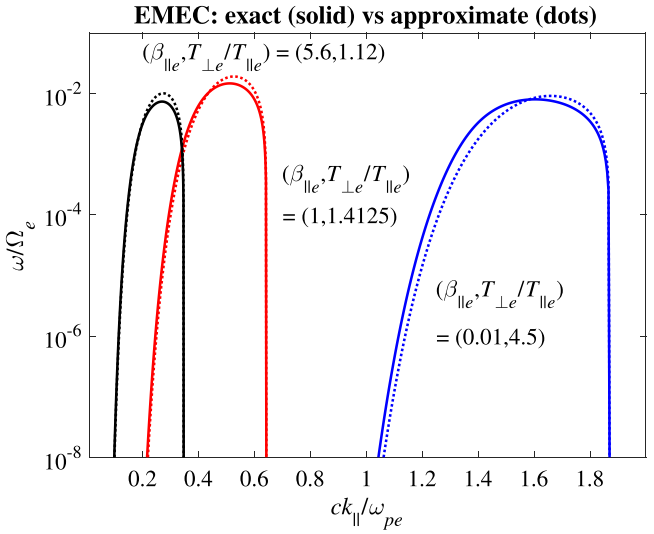

FIG. 4. Exact (solid lines) *versus* approximate (dotted lines) growth rates of EMEC instability, γ/Ω_i *versus* $ck_\|/\omega_{pi}$, for $(\beta_{\|e},T_{\perp e}/T_{\|e}) = (0.01, 4.5)$ (blue), $(\beta_{\|e},T_{\perp e}/T_{\|e}) = (1, 1.4125)$ (red), and $(\beta_{\|e},T_{\perp e}/T_{\|e}) = (5.6, 1.12)$ (black).

numerical examples will be based on the three combinations of parallel beta and temperature ratios for each EMIC and EMEC instabilities, as indicated in Figs. 1 and 2, and analyzed specifically in Figs. 3 and 4.

B. Weakly growing low frequency EMIC instability

In order to proceed, we resort to the cold plasma theory for the determination of real frequency, and make use of the customary method to calculate the weak growth/damping rate. For cold plasma and for low frequency, we may approximate the dielectric tensor elements by

$$\begin{aligned}\epsilon_{xx} &= \frac{\omega_{pi}^2}{\Omega_i^2-\omega^2} = \epsilon_{yy},\\ \epsilon_{xy} &= \frac{i\omega}{\Omega_i}\frac{\omega_{pi}^2}{\Omega_i^2-\omega^2} = -\epsilon_{yx},\\ \epsilon_{zz} &= -\frac{\omega_{pe}^2}{\omega^2},\end{aligned} \tag{5}$$

and $\epsilon_{xz} = \epsilon_{zx} = \epsilon_{yz} = -\epsilon_{zy} = 0$. Note that the leading component is the ϵ_{zz}. The dispersion relation is thus given by

$$\begin{aligned}0 = {}& N^4\left(\epsilon_{xx}\sin^2\theta + \epsilon_{zz}\cos^2\theta\right)\\ & -N^2\left[2\epsilon_{xx}\epsilon_{zz} + \left(\epsilon_{xx}^2+\epsilon_{xy}^2-\epsilon_{xx}\epsilon_{zz}\right)\sin^2\theta\right]\\ & +\left(\epsilon_{xx}^2+\epsilon_{xy}^2\right)\epsilon_{zz},\end{aligned} \tag{6}$$

where $N = ck/\omega$ is the index of refraction and θ represents the angle between the wave vector and the ambient magnetic field. Since ϵ_{zz} is the dominant term, we may approximate the full dispersion relation (6) by retaining only those terms associated with the leading term

$$0 = N^4\cos^2\theta - N^2\frac{\omega_{pi}^2(2-\sin^2\theta)}{\Omega_i^2-\omega^2} + \frac{\omega_{pi}^4}{\Omega_i^2\left(\Omega_i^2-\omega^2\right)}. \tag{7}$$

This equation can be solved either for N^2, in which case we have

$$\begin{aligned}N^2 &= \frac{\omega_{pi}^2}{\Omega_i(\Omega_i-\tau\omega)},\\ \tau &= s+\sqrt{s^2+\cos^2\theta}, \quad s = \frac{\Omega_i\sin^2\theta}{2\omega},\end{aligned} \tag{8}$$

or in terms of ω^2. In the latter case, we obtain

$$\begin{aligned}\frac{\omega^2}{\Omega_i^2} = \frac{1}{2}\frac{c^2k^2}{\omega_{pi}^2}\Bigg\{1+\left(1+\frac{c^2k^2}{\omega_{pi}^2}\right)\cos^2\theta\\ -\left[1+\left(1+\frac{c^2k^2}{\omega_{pi}^2}\right)^2\cos^4\theta - 2\left(1-\frac{c^2k^2}{\omega_{pi}^2}\right)\cos^2\theta\right]^{1/2}\Bigg\}.\end{aligned} \tag{9}$$

Note that the solution (8) is reminiscent of the magnetoionic dispersion relation.[23] In the customary magnetoionic theory,

the low frequency modes associated with the ion response are ignored.

Following the customary practice exercised in the magnetoionic theory,[23] it is useful to define the unit electric field vector

$$\begin{aligned}\hat{\mathbf{e}}(\mathbf{k}) &= \frac{\delta\mathbf{E}(\mathbf{k})}{|\delta\mathbf{E}(\mathbf{k})|} = \frac{K\hat{\kappa} + T\hat{t} + i\hat{a}}{(K^2+T^2+1)^{1/2}},\\ \hat{\kappa} &= (\sin\theta,\ 0,\ \cos\theta),\\ \hat{a} &= (0,\ 1,\ 0),\\ \hat{t} &= (\cos\theta,\ 0,\ -\sin\theta).\end{aligned} \tag{10}$$

Representing the unit electric field in the above form is useful since the coefficients K and T define the polarization characteristics of a given wave mode. In particular, if $K=\infty$ then the mode is a purely longitudinal (electrostatic) mode. If, on the other hand, $K=0$ then the mode is a pure transverse electromagnetic mode. If $K=$ finite but $T=\infty$, then such a mode is also a purely transverse mode. In order to determine the specific expressions for K and T, we make use of the cold plasma dispersion relation. For the present case of low frequency, the cold plasma EMIC mode, it can be shown, after some considerations, that K and T are given by

$$K = -\frac{\tau\sin\theta}{\cos^2\theta}, \quad \text{and} \quad T = -\frac{\tau}{\cos\theta}, \tag{11}$$

where τ is defined in Eq. (8). These quantities will be useful for the computation of the growth/damping rates of weakly unstable modes.

The growth/damping rate can be determined on the basis of the linear dielectric response tensor, which is given by

$$\begin{aligned}\epsilon_{ij}(\mathbf{k},\omega) &= \delta_{ij} + \sum_a \frac{\omega_{pa}^2}{\omega^2}\int d\mathbf{v}\left[\frac{v_\parallel}{v_\perp}\left(v_\perp\frac{\partial}{\partial v_\parallel} - v_\parallel\frac{\partial}{\partial v_\perp}\right)f_a b_i b_j\right.\\ &\left. + \sum_{n=-\infty}^{\infty}\frac{V_i V_j^*}{\omega - n\Omega_a - k_\parallel v_\parallel}\left(\frac{\omega - k_\parallel v_\parallel}{v_\perp}\frac{\partial}{\partial v_\perp} + k_\parallel\frac{\partial}{\partial v_\parallel}\right)f_a\right],\\ V_i &= \left(v_\perp\frac{nJ_n(b)}{b}, -iv_\perp J_n'(b), v_\parallel J_n(b)\right),\end{aligned} \tag{12}$$

where $b = k_\perp v_\perp/\Omega_a$, $k_\parallel = k\cos\theta$, $k_\perp = k\sin\theta$, the summation over a represents sum over charged particle species, f_a denotes the particle velocity distribution function, normalized to unity ($\int d\mathbf{v} f_a = 1$), and $J_n(b)$ is the Bessel function of the first kind of order n. The unit vector $b_i = (\mathbf{B}_0)_j/B_0$ is simply $\hat{z}$, since we assumed that the ambient magnetic field lies along the z axis. The generic form of the linear wave equation is given by

$$\left[\epsilon_{ij}^H + \epsilon_{ij}^A - N^2\left(\delta_{ij} - \frac{k_i k_j}{k^2}\right)\right]\delta E_j = 0, \tag{13}$$

where the dielectric response tensor is written as a sum of the hermitian and anti-hermitian parts, where these quantities are defined by $\epsilon_{ij}^H(\mathbf{k},\omega) = \frac{1}{2}[\epsilon_{ij}(\mathbf{k},\omega) + \epsilon_{ij}^*(\mathbf{k},\omega)]$, and $\epsilon_{ij}^A(\mathbf{k},\omega) = \frac{1}{2}[\epsilon_{ij}(\mathbf{k},\omega) - \epsilon_{ij}^*(\mathbf{k},\omega)]$, or written explicitly,

$$\begin{aligned}\epsilon_{ij}^H &= \delta_{ij} + \sum_a \frac{\omega_{pa}^2}{\omega^2}\int d\mathbf{v}\left[\left(\frac{1}{2}(\delta_{ij} - b_i b_j)v_\perp\frac{\partial}{\partial v_\perp} + b_i b_j v_\parallel\frac{\partial}{\partial v_\parallel}\right)f_a\right.\\ &\left. + \sum_{n=-\infty}^{\infty}\mathcal{P}\frac{V_i V_j^*}{\omega - n\Omega_a - k_\parallel v_\parallel}\left(\frac{n\Omega_a}{v_\perp}\frac{\partial}{\partial v_\perp} + k_\parallel\frac{\partial}{\partial v_\parallel}\right)f_a\right],\\ \epsilon_{ij}^A &= -i\sum_a\frac{\omega_{pa}^2}{\omega^2}\int d\mathbf{v}\sum_{n=-\infty}^{\infty}V_i V_j^*\delta(\omega - n\Omega_a - k_\parallel v_\parallel)\\ &\times\left(\frac{n\Omega_a}{v_\perp}\frac{\partial}{\partial v_\perp} + k_\parallel\frac{\partial}{\partial v_\parallel}\right)f_a.\end{aligned} \tag{14}$$

In the above, $\mathcal{P}$ denotes the principal value.

Writing the wave electric field in terms of the unit vector $\hat{e}_i$ introduced before, namely, $\delta E_j = \hat{e}_j\,\delta E$, we may express the linear wave equation by multiplying ω^2 to both sides of the equation and by taking an inner product with $\hat{e}_i^*$,

$$\hat{e}_i^*\left[\omega^2\,\epsilon_{ij}^H - \omega^2 N^2\left(\delta_{ij} - \frac{k_i k_j}{k^2}\right)\right]\hat{e}_j + \omega^2\hat{e}_i^*\epsilon_{ij}^A\hat{e}_j = 0. \tag{15}$$

If we write the complex frequency as $\omega = \omega_r + i\gamma$, and make use of the fact that the plasma normal mode satisfies the dispersion relation, which is the first term on the left-hand side of (15), then upon expanding Eq. (15) as a Taylor series we obtain

$$\frac{\gamma}{\omega} = \frac{i\hat{e}_i^*\epsilon_{ij}^A\hat{e}_j}{\omega^{-1}\left[\partial(\omega^2\epsilon)/\partial\omega\right]}, \quad \epsilon = \hat{e}_i^*\epsilon_{ij}^H\hat{e}_j. \tag{16}$$

where ω is meant to be the real part of the complex frequency, $\omega = \omega_r$, and the unit electric field vector $\hat{e}_i$ is defined in Eq. (10). Making explicit use of Eq. (12), we obtain the expression for the growth rate

$$\begin{aligned}\gamma &= \sum_a\frac{\omega_{pa}^2}{\partial\left[\omega^2\epsilon(\mathbf{k},\omega)\right]/\partial\omega}\int d\mathbf{p}\sum_{n=-\infty}^{\infty}|\hat{\mathbf{e}}^*(\mathbf{k})\cdot\mathbf{V}|^2\\ &\times\delta(\omega - n\Omega_a - k_\parallel v_\parallel)\left(\frac{n\Omega_a}{\gamma v_\perp}\frac{\partial}{\partial v_\perp} + k_\parallel\frac{\partial}{\partial v_\parallel}\right)f_a.\end{aligned} \tag{17}$$

In the above, the quantity in the denominator, $\partial(\omega^2\epsilon)/\partial\omega$, can be computed as follows:

$$\begin{aligned}\frac{\partial}{\partial\omega}(\omega^2\epsilon) &= \frac{\partial}{\partial\omega}\left[\omega^2\hat{e}_i^*\epsilon_{ij}^H\hat{e}_j\right]\\ &= \left(1 - \frac{|\hat{\mathbf{e}}(\mathbf{k})\cdot\mathbf{k}|^2}{k^2}\right)2\omega\,\frac{\partial(\omega^2N^2)}{\partial\omega^2}\\ &= \frac{1+T^2}{1+K^2+T^2}\,2\omega\,\frac{\partial(\omega^2N^2)}{\partial\omega^2},\end{aligned} \tag{18}$$

where we have made use of the dispersion relation and Eq. (10). The remaining quantity of interest is $\partial(\omega^2N^2)/\partial\omega^2$, which upon making use of N^2 defined in Eq. (8), can be shown to reduce to

$$R \equiv \frac{\partial(\omega^2N^2)}{\partial\omega^2} = \frac{\omega_{pi}^2}{\Omega_i^2 - \omega^2}\left(\frac{\Omega_i}{\Omega_i - \tau\omega} + \frac{\omega}{\Omega_i}\frac{1}{\sin^2\theta}\frac{\tau^2 - \cos^2\theta}{\tau^2 + \cos^2\theta}\right). \tag{19}$$

Upon making use of the definition for $\hat{\mathbf{e}}$ in (10), the final explicit expression for the growth/damping rate emerges

$$\gamma = \frac{\pi}{2\omega}\sum_a \frac{\omega_{pa}^2}{(1+T^2)R}\int d\mathbf{v}\, v_\perp^2 \sum_{n=-\infty}^{\infty} \times \left\{\frac{\omega}{\Omega_a}\left[K\sin\theta + T\left(\cos\theta - \frac{kv_\parallel}{\omega}\right)\right]\frac{J_n(b)}{b} - J_n'(b)\right\}^2 \times \delta\left(\omega - n\Omega_a - k_\parallel v_\parallel\right)\left(\frac{n\Omega_a}{v_\perp}\frac{\partial}{\partial v_\perp} + k_\parallel \frac{\partial}{\partial v_\parallel}\right) f_a(v_\perp^2, v_\parallel). \tag{20}$$

Let us assume the bi-Maxwellian velocity distribution function

$$f_i = \frac{1}{\pi^{3/2}\alpha_{\perp i}^2\alpha_{\parallel i}}\exp\left(-\frac{v_\perp^2}{\alpha_{\perp i}^2} - \frac{v_\parallel^2}{\alpha_{\parallel i}^2}\right), \quad \alpha_{\perp i}^2 = \frac{2T_{\perp i}}{m_i}, \quad \alpha_{\parallel i}^2 = \frac{2T_{\parallel i}}{m_i}. \tag{21}$$

Let us also make specific use of K and T for the EMIC mode—see Eq. (11). Upon making use of the above assumptions and implementing various approximation procedures, it is possible to carry out the velocity integrals in the closed form by means of the well known Bessel function integral formulae and by virtue of the delta function resonance condition. The result is as follows:

$$\gamma = \frac{\pi^{1/2}}{2\tilde{R}}\frac{\Omega_i^2 - \omega^2}{\omega|k_\parallel|\alpha_{\parallel i}}\sum_{n=-\infty}^{\infty}\left((\tau^2 + \cos^4\theta)\frac{n^2 I_n(\lambda)e^{-\lambda}}{\lambda} + 2(n\tau - \lambda\cos^2\theta)\cos^2\theta\frac{d\left[I_n(\lambda)e^{-\lambda}\right]}{d\lambda}\right) \times \left[\left(\frac{T_{\perp i}}{T_{\parallel i}} - 1\right)n\Omega_i - \frac{T_{\perp i}}{T_{\parallel i}}\omega\right]e^{-\zeta^2},$$
$$\zeta = \frac{n\Omega_i - \omega}{k_\parallel\alpha_{\parallel i}}, \quad \lambda = \frac{k_\perp^2\alpha_{\perp i}^2}{2\Omega_i^2},$$
$$\tilde{R} = \frac{\Omega_i\cos^2\theta}{\Omega_i - \tau\omega}(\tau^2 + \cos^2\theta) + \frac{\omega\cos^2\theta}{\Omega_i\sin^2\theta}(\tau^2 - \cos^2\theta). \tag{22}$$

In the above, $I_n(\lambda)$ is the modified Bessel function of the first kind of order 1. The real frequency ω is given by Eq. (9). The quantity τ is defined in Eq. (8). This is the desired growth rate for EMIC instability.

C. Weakly growing high frequency EMEC instability

For EMEC wave and instability, the customary magneto-ionic theory is applicable. Since the whistler mode or the EMEC mode is a slow mode, we may ignore the displacement current. The non-vanishing components of the cold plasma dielectric tensor ignoring the ion response are given by

$$\epsilon_{xx} = \frac{\omega_{pe}^2}{\Omega_e^2 - \omega^2} = \epsilon_{yy}, \quad \epsilon_{xy} = \frac{i\Omega_e}{\omega}\frac{\omega_{pe}^2}{\Omega_e^2 - \omega^2} = -\epsilon_{yx}, \quad \epsilon_{zz} = -\frac{\omega_{pe}^2}{\omega^2}. \tag{23}$$

The dispersion equation can be obtained exactly on the basis of the above approximations either in terms N^2

$$N^2 = \frac{\omega_{pe}^2}{\omega(\Omega_e\cos\theta - \omega)}, \tag{24}$$

or conversely, in terms of ω

$$\omega = \Omega_e\cos\theta\,\frac{c^2k^2/\omega_{pe}^2}{1 + c^2k^2/\omega_{pe}^2}. \tag{25}$$

For the whistler mode branch, the following coefficients K and T for the unit polarization vector as well as the quantity R can be derived

$$K = -\frac{\Omega_e\sin\theta}{\Omega_e\cos\theta - \omega}, \quad T = -1,$$
$$R = \frac{\partial(\omega^2N^2)}{\partial\omega^2} = \frac{\partial(\omega^2N^2)}{\partial\omega^2} = \frac{\omega_{pe}^2\Omega_e\cos\theta}{2\omega(\Omega_e\cos\theta - \omega)^2}. \tag{26}$$

From the general growth/damping rate expression (20), we again consider bi-Maxwellian distribution of electrons and ignore ions. Then, the EMEC instability growth rate is given by

$$\gamma = \frac{\pi^{1/2}}{2}\frac{\cos\theta - \omega/\Omega_e}{\cos^3\theta}\sum_{n=-\infty}^{\infty}\left\{\left[\left(\frac{\omega^2\sin^2\theta}{\Omega_e(\Omega_e\cos\theta - \omega)} + n\right)^2 + n^2\cos^2\theta\right]\frac{I_n(\lambda)e^{-\lambda}}{\lambda} + 2\cos\theta\left(\frac{\omega^2\sin^2\theta}{\Omega_e(\Omega_e\cos\theta - \omega)} + n - \lambda\cos\theta\right)\frac{d\left[I_n(\lambda)e^{-\lambda}\right]}{d\lambda}\right\} \times \left[\frac{T_{\perp e}}{T_{\parallel e}}\frac{\omega}{\Omega_e} - \left(\frac{T_{\perp e}}{T_{\parallel e}} - 1\right)n\right]\frac{\Omega_e e^{-\zeta^2}}{k_\parallel\alpha_{\parallel e}},$$
$$\zeta = \frac{\omega - n\Omega_e}{k_\parallel\alpha_{\parallel e}}, \quad \lambda = \frac{k_\perp^2\alpha_{\perp e}^2}{2\Omega_e^2}. \tag{27}$$

This is the desired growth rate expression for EMEC instability, which is valid under the assumption of weak growth and for the bi-Maxwellian electron distribution function. In Sec. IV, we will discuss the numerical calculation of EMIC and EMEC instability growth rates based upon Eqs. (22) and (27), respectively, but it turns out that all other harmonic terms except $n = 0$ and 1 terms are unimportant.

III. QUASILINEAR THEORY OF CYCLOTRON INSTABILITIES IN THE LOW β REGIME

The convenient starting point for the present section is the well-known quasilinear velocity space diffusion equation[24]

$$\frac{\partial f_a}{\partial t} = \frac{\pi e_a^2}{m_a^2}\sum_{n=-\infty}^{\infty}\int d\mathbf{k}\left[\left(1 - \frac{k_\parallel v_\parallel}{\omega}\right)\frac{\partial}{v_\perp\partial v_\perp} + \frac{k_\parallel}{\omega}\frac{\partial}{\partial v_\parallel}\right] \times \langle|\mathbf{V}^{n*}\cdot\delta\mathbf{E}_\mathbf{k}|^2\rangle\delta(\omega - n\Omega_a - k_\parallel v_\parallel) \times \left[\left(1 - \frac{k_\parallel v_\parallel}{\omega}\right)\frac{\partial}{v_\perp\partial v_\perp} + \frac{k_\parallel}{\omega}\frac{\partial}{\partial v_\parallel}\right] f_a. \tag{28}$$

In the present approach, we do not actually solve the above kinetic directly for f_a, but rather we take the simple

and approximate approach. This is the method employed by Ref. 19, and it is a reduced quasilinear theory. The method involved taking the velocity moments, $T_{\perp a} = (m_a/2)\int d\mathbf{v} v_\perp^2 f_a$ and $T_{\parallel a} = m_a \int d\mathbf{v} v_\parallel^2 f_a$, of Eq. (28), under the assumption that f_a is given by the bi-Maxwellian form (21) for all time, except that the temperatures evolve in time. Of course, this is an approximation that must be employed judiciously depending on the nature of the instability. For the present cyclotron instabilities, it was already shown by direct comparison with the particle-in-cell or Vlasov simulation that the present approach is valid at least as a first-cut approach.[25–27] The approximate validity of the bi-Maxwellian assumption (or lack thereof) is demonstrated by the particle-in-cell simulation of weakly growing EMEC instability in the low beta regime by Gary *et al.*[4] In their simulation, the nonlinear development of the electron distribution function along $v_\perp$ is presumably quasi Maxwellian for all time, but along $v_\parallel$, it was shown that energetic "shoulder" is formed for later times. However, the bulk of the electron population is still represented by the Maxwellian form. Note that Fig. 7 of Ref. 4 is plotted in the vertical logarithmic scale such that the deviation from the Maxwellian form is over-emphasized. Reference 27, on the other hand, carried out particle-in-cell simulation of EMEC instability for moderately low beta and showed that the quasi bi-Maxwellian nature of the electron distribution is well maintained for all time – see Fig. 3 of their paper. These simulation results provide some justifications for the present approach of bi-Maxwellian assumption for all time, at least as a first cut method. We thus take the velocity moments of Eq. (28) and make use of the unit electric field vector (10). This leads to

$$\frac{dT_{\perp a}}{dt} = -\frac{\pi e_a^2}{m_a}\sum_{n=-\infty}^{\infty}\int d\mathbf{k}\langle \delta E_{\mathbf{k}}^2\rangle \int d\mathbf{v}\left(1-\frac{k_\parallel v_\parallel}{\omega}\right)H_n,$$

$$\frac{dT_{\parallel a}}{dt} = -\frac{2\pi e_a^2}{m_a}\sum_{n=-\infty}^{\infty}\int d\mathbf{k}\langle \delta E_{\mathbf{k}}^2\rangle \int d\mathbf{v}\,\frac{k_\parallel v_\parallel}{\omega}\,H_n,$$

$$H_n = \frac{1}{1+K^2+T^2}\left\{\frac{\omega}{\Omega_a}\left[K\sin\theta + T\left(\cos\theta - \frac{kv_\parallel}{\omega}\right)\right]\right.$$
$$\left.\times\frac{J_n(b)}{b} - \frac{dJ_n(b)}{db}\right\}^2 \times v_\perp^2\,\delta(\omega - n\Omega_a - k_\parallel v_\parallel)$$
$$\times\left[\left(1-\frac{k_\parallel v_\parallel}{\omega}\right)\frac{\partial}{v_\perp\partial v_\perp} + \frac{k_\parallel}{\omega}\frac{\partial}{\partial v_\parallel}\right] f_a. \tag{29}$$

Another caveat concerning the present approach is that Eq. (28) is based upon the implicit assumption that the instability is weakly growing such that the growth/damping rate is considered much lower than the real frequency, $\gamma \ll \omega$. Such an assumption is valid for weakly growing cyclotron instabilities, which are the subject of the present analysis. However, for mirror instability, which is aperiodic, $\omega = 0$, the quasilinear diffusion equation of the type (28) is not applicable. Consequently, in a recent work,[7] where we considered the weakly growing mirror instability, the full resonance condition in the quasilinear kinetic equation was adopted before we took the velocity moments.

For bi-Maxwellian f_a given by (21), and carrying out the velocity integral, we have

$$\frac{dT_{\perp a}}{dt} = \frac{\pi^{1/2}e_a^2}{m_a}\sum_{n=-\infty}^{\infty}\int d\mathbf{k}\langle \delta E_{\mathbf{k}}^2\rangle \frac{n\Omega_a}{\omega}H_n,$$

$$\frac{dT_{\parallel a}}{dt} = \frac{2\pi^{1/2}e_a^2}{m_a}\sum_{n=-\infty}^{\infty}\int d\mathbf{k}\langle \delta E_{\mathbf{k}}^2\rangle \left(1-\frac{n\Omega_a}{\omega}\right)H_n,$$

$$H_n = \frac{1}{1+K^2+T^2}\left[\frac{T_{\perp a}}{T_{\parallel a}} - \left(\frac{T_{\perp a}}{T_{\parallel a}}-1\right)\frac{n\Omega_a}{\omega}\right]\frac{e^{-\left(\zeta_n^a\right)^2}}{|k_\parallel \alpha_{\parallel a}|}$$
$$\times\left(\left\{\frac{\omega^2}{\Omega_a^2}\left[K\sin\theta + \frac{T}{\cos\theta}\left(\frac{n\Omega_a}{\omega}-\sin^2\theta\right)\right]^2 + n^2\right\}\right.$$
$$\times\frac{I_n(\lambda_a)e^{-\lambda_a}}{\lambda_a} - 2\left\{\frac{\omega}{\Omega_a}\left[K\sin\theta + \frac{T}{\cos\theta}\left(\frac{n\Omega_a}{\omega}-\sin^2\theta\right)\right]\right.$$
$$\left.\left.+\lambda_a\right\}\frac{d\left[I_n(\lambda_a)e^{-\lambda_a}\right]}{d\lambda_a}\right),$$
$$\lambda_a = \frac{k_\perp^2\alpha_{\perp a}^2}{2\Omega_a^2}, \quad \zeta_n^a = \frac{\omega - n\Omega_a}{k_\parallel\alpha_{\parallel a}}. \tag{30}$$

Note that the definition for H_n in Eq. (29) is different from Eq. (30).

A. Quasilinear moment theory of weakly growing EMIC instability for Bi-Maxwellian temperatures

For the EMIC mode, we make use of the dispersion relation (9) and the definition (11). Restricting to protons in Eq. (30), we obtain explicit expressions as given below. In the following results, however, we have retained harmonic contributions from $n = 0$ and 1 terms only, since these are the only terms that have finite contributions. We have checked this by including other harmonic terms also but found no difference from the result in which only $n = 0$ and 1 terms are retained. The results are thus given by

$$\frac{dT_{\perp i}}{dt} = -\frac{\pi^{1/2}e^2}{m_i}\int d\mathbf{k}\,\frac{\langle \delta E_{\mathbf{k}}^2\rangle}{\tau^2+\cos^4\theta}\frac{\Omega_i}{\omega}H_1,$$

$$\frac{dT_{\parallel i}}{dt} = \frac{2\pi^{1/2}e^2}{m_i}\int d\mathbf{k}\,\frac{\langle \delta E_{\mathbf{k}}^2\rangle}{\tau^2+\cos^4\theta}\left[H_0 + \left(\frac{\Omega_i}{\omega}-1\right)H_1\right],$$

$$H_0 = \frac{T_{\perp i}}{T_{\parallel i}}\,2\lambda[I_0(\lambda)-I_1(\lambda)]e^{-\lambda}\,\frac{\exp(-\xi^2)}{|k_\parallel\alpha_{\parallel i}|},$$

$$H_1 = \left[\left(\frac{T_{\perp i}}{T_{\parallel i}}-1\right)\frac{\Omega_i}{\omega} - \frac{T_{\perp i}}{T_{\parallel i}}\right]\left(\frac{I_1(\lambda)e^{-\lambda}}{\lambda}\,(\tau^2+\cos^4\theta)\right.$$
$$\left.+2\,\frac{d\left[I_1(\lambda)e^{-\lambda}\right]}{d\lambda}\,(\tau-\lambda\cos^2\theta)\cos^2\theta\right)\frac{\exp(-\zeta^2)}{|k_\parallel\alpha_{\parallel i}|},$$
$$\lambda = \frac{k_\perp^2\alpha_{\perp i}^2}{2\Omega_i^2}, \quad \zeta = \frac{\omega-\Omega_i}{k_\parallel\alpha_{\parallel i}}, \quad \xi = \frac{\omega}{k_\parallel\alpha_{\parallel i}}. \tag{31}$$

The wave kinetic equation is simply given by the customary form, $\partial\langle\delta E_{\mathbf{k}}^2\rangle/\partial t = 2\gamma_{\mathbf{k}}\langle\delta E_{\mathbf{k}}^2\rangle$.

B. Quasilinear moment theory of weakly growing EMEC instability for Bi-Maxwellian temperatures

For the weakly growing EMEC case, we restrict Eq. (30) to the electrons and retain only $n = 0$ and 1 terms (again, we have verified that other terms make no contributions)

$$\frac{dT_{\perp e}}{dt} = \frac{\pi^{1/2}e^2}{m_e\Omega_e}\int d\mathbf{k}\,\frac{\Omega_e}{\omega}\,GH_1\langle\delta E_{\mathbf{k}}^2\rangle,$$

$$\frac{dT_{\parallel e}}{dt} = \frac{2\pi^{1/2}e^2}{m_e\Omega_e}\int d\mathbf{k}\left(1-\frac{n\Omega_e}{\omega}\right)G(H_0+H_1)\langle\delta E_{\mathbf{k}}^2\rangle,$$

$$G = \frac{\Omega_e}{\omega}\frac{1}{\cos^2\theta}\frac{(\cos\theta-\omega/\Omega_e)^2}{2(\cos\theta-\omega/\Omega_e)^2+\sin^2\theta},$$

$$L = \frac{\omega^2\sin^2\theta}{\Omega_e^2(\cos\theta-\omega/\Omega_e)},$$

$$H_0 = \left\{L^2\frac{I_0(\lambda)e^{-\lambda}}{\lambda}+2\cos\theta(L-\lambda\cos\theta)\frac{d\left[I_0(\lambda)e^{-\lambda}\right]}{d\lambda}\right\}\times\frac{T_{\perp e}}{T_{\parallel e}}\,\xi\exp\left(-\xi^2\right),$$

$$H_1 = \left\{\left[(L+1)^2+\cos^2\theta\right]\frac{I_1(\lambda)e^{-\lambda}}{\lambda}+2\cos\theta(L+1-\lambda\cos\theta)\frac{d\left[I_1(\lambda)e^{-\lambda}\right]}{d\lambda}\right\}\times\left[\frac{T_{\perp e}}{T_{\parallel e}}\frac{\omega}{\Omega_e}-\left(\frac{T_{\perp e}}{T_{\parallel e}}-1\right)\right]\frac{\Omega_e\exp\left(-\zeta^2\right)}{k\alpha_{\parallel e}\cos\theta},$$

$$\xi = \frac{\omega}{k_\parallel\alpha_{\parallel e}},\quad \zeta = \frac{\omega-\Omega_e}{k_\parallel\alpha_{\parallel e}},\quad \lambda = \frac{k_\perp^2\alpha_{\perp e}^2}{2\Omega_e^2}. \tag{32}$$

The wave kinetic equation for the EMEC wave is also given by the standard form, $\partial\langle\delta E_{\mathbf{k}}^2\rangle/\partial t = 2\gamma_{\mathbf{k}}\langle\delta E_{\mathbf{k}}^2\rangle$.

IV. NUMERICAL EXAMPLES

On the basis of the analytical theory of cyclotron instabilities developed in Secs. II and III, we now consider 2D EMIC and 2D EMEC instabilities for sample weakly growing cases indicated in Figs. 1 and 2. In the present calculation, we have checked the conservation of total energy. The particle plus field energy is given by

$$\mathscr{E} = \sum_a\frac{nm_a}{2}\int d\mathbf{v}\,v_\perp^2 f_a+\frac{nm_a}{2}\int d\mathbf{v}\,v_\parallel^2 f_a+\int d\mathbf{k}\,\frac{\langle\delta E_{\mathbf{k}}^2\rangle}{B_0^2}+\int d\mathbf{k}\,\frac{\langle\delta B_{\mathbf{k}}^2\rangle}{B_0^2}+\frac{B_0^2}{8\pi}. \tag{33}$$

First we discuss the EMIC instability. We solved Eq. (31) for the evolution of temperatures, or equivalently, the betas, $\beta_{\perp i} = 8\pi n_0 T_{\perp i}/B_0^2$ and $\beta_{\parallel i} = 8\pi n_0 T_{\parallel i}/B_0^2$. In Fig. 5, we plot the result of quasilinear calculation. For case 1, we chose the initial input parameters corresponding to $[\beta_{\parallel i}(0), T_{\perp i}(0)/T_{\parallel i}(0)] = (0.1, 2.24)$. Case 2 parameters are $[\beta_{\parallel i}(0), T_{\perp i}(0)/T_{\parallel i}(0)] = (1, 1.52)$, while for case 3, the initial parameters are $[\beta_{\parallel i}(0), T_{\perp i}(0)/T_{\parallel i}(0)] = (6.3, 1.15)$. The

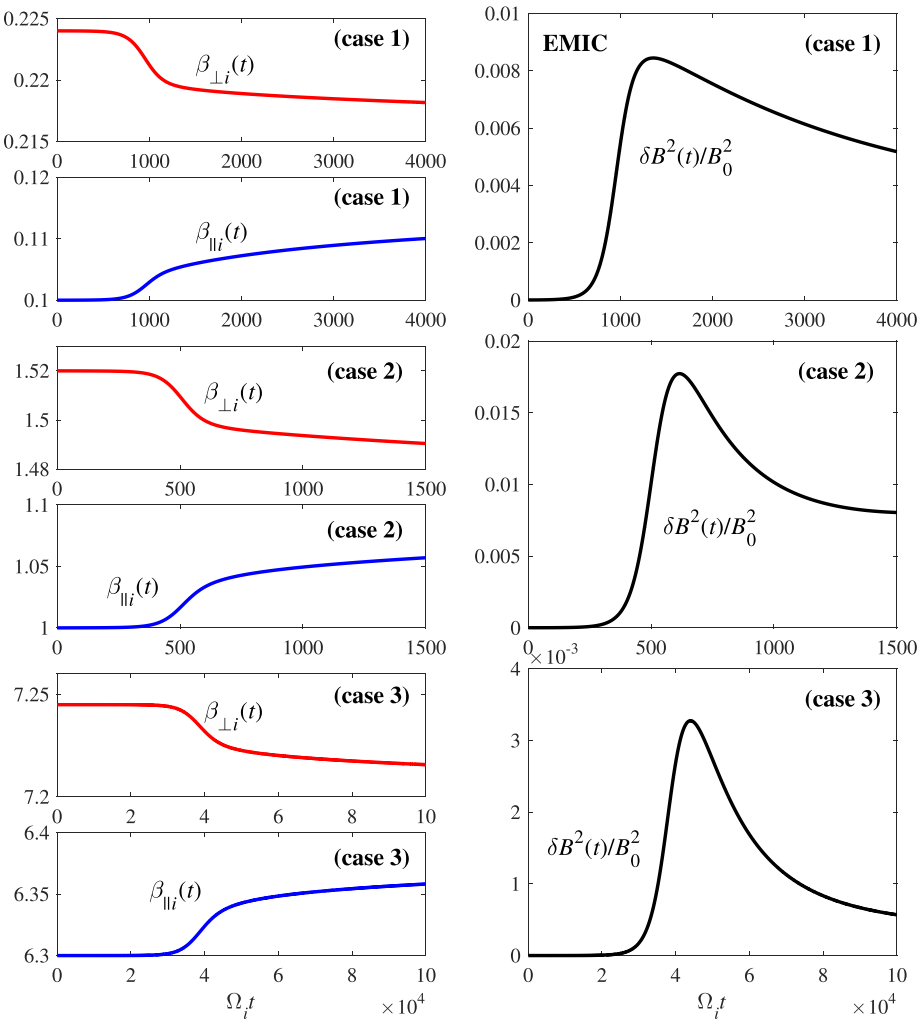

FIG. 5. Time evolution of $\beta_{\perp i}(t)$ and $\beta_{\parallel i}(t)$ [left] and normalized wave magnetic field energy density $\delta B^2(t)/B_0^2$ associated with EMIC instability [right] *versus* normalized time $\Omega_i t$, for initial conditions (case 1) $\beta_{\parallel i} = 0.1$ and $T_{\perp i}/T_{\parallel i} = 2.24$, (case 2) $\beta_{\parallel i} = 1$ and $T_{\perp i}/T_{\parallel i} = 1.52$, and (case 3) $\beta_{\parallel i} = 6.3$ and $T_{\perp i}/T_{\parallel i} = 1.15$.

left-hand panels plot the perpendicular and parallel proton betas, $\beta_{\perp i}(t)$ and $\beta_{\|i}(t)$, *versus* normalized time Ω_{it}, and on the right, normalized wave magnetic field energy density associated with the EMIC instability

$$\frac{\delta B^2(t)}{B_0^2} = \int d\mathbf{k}\, \frac{c^2k^2}{\omega_{\mathbf{k}}^2} \frac{\langle \delta E_{\mathbf{k}}^2 \rangle}{B_0^2}, \tag{34}$$

is plotted *versus* Ω_{it}. In all the cases we ran, the total energy (33) is conserved.

It can be seen that the free energy source, that is, the excessive perpendicular temperature anisotropy, is reduced as EMIC instability is excited, but the time scales are vastly different for three cases. The perpendicular beta is reduced while the parallel beta increases in all three cases. The wave energy density first exponentially increases, followed by saturation, but after the wave intensity reaches the peak, the net energy density decreases again. This is owing to the reabsorption of the wave energy by the particles as the range of unstable mode generally shrinks in size.

Figure 6 represents the snapshots of the growth rate, $\gamma_{\mathbf{k}}/\Omega_i$, for the three sample cases shown in Fig. 7, each at different time intervals. The color bar indicates the magnitude of the growth rate. As the instability progresses, the instantaneous growth rate is reduced for each case, as can be judged from the color bar. Also the unstable range of wave numbers shrinks as the system approaches saturation. Note that for the right-hand panels (case 3), the x axis is defined over a very small perpendicular wave number range, $10^{-3} < ck_\perp/\omega_{pi} < 4 \times 10^{-3}$, which is indicated in the axis labels with an overall multiplicative factor $\times 10^{-3}$.

For EMEC, as noted in the Introduction, in the low beta regime, the maximum growth rate shifts from the quasi parallel direction to oblique propagation angles.[3,4] The analytical growth rate formula (27) reproduces this behavior. Figure 7 is the result of quasilinear calculation based upon Eq. (32). We plot the evolution of normalized temperatures, or equivalently, the electron betas, $\beta_{\perp e} = 8\pi n_0 T_{\perp e}/B_0^2$ and $\beta_{\|e} = 8\pi n_0 T_{\|e}/B_0^2$, *versus* normalized time Ω_{et}. In Fig. 7, the left-hand panels plot $\beta_{\perp e}(t)$ and $\beta_{\|e}(t)$ for three different initial values of parallel betas and temperature anisotropies

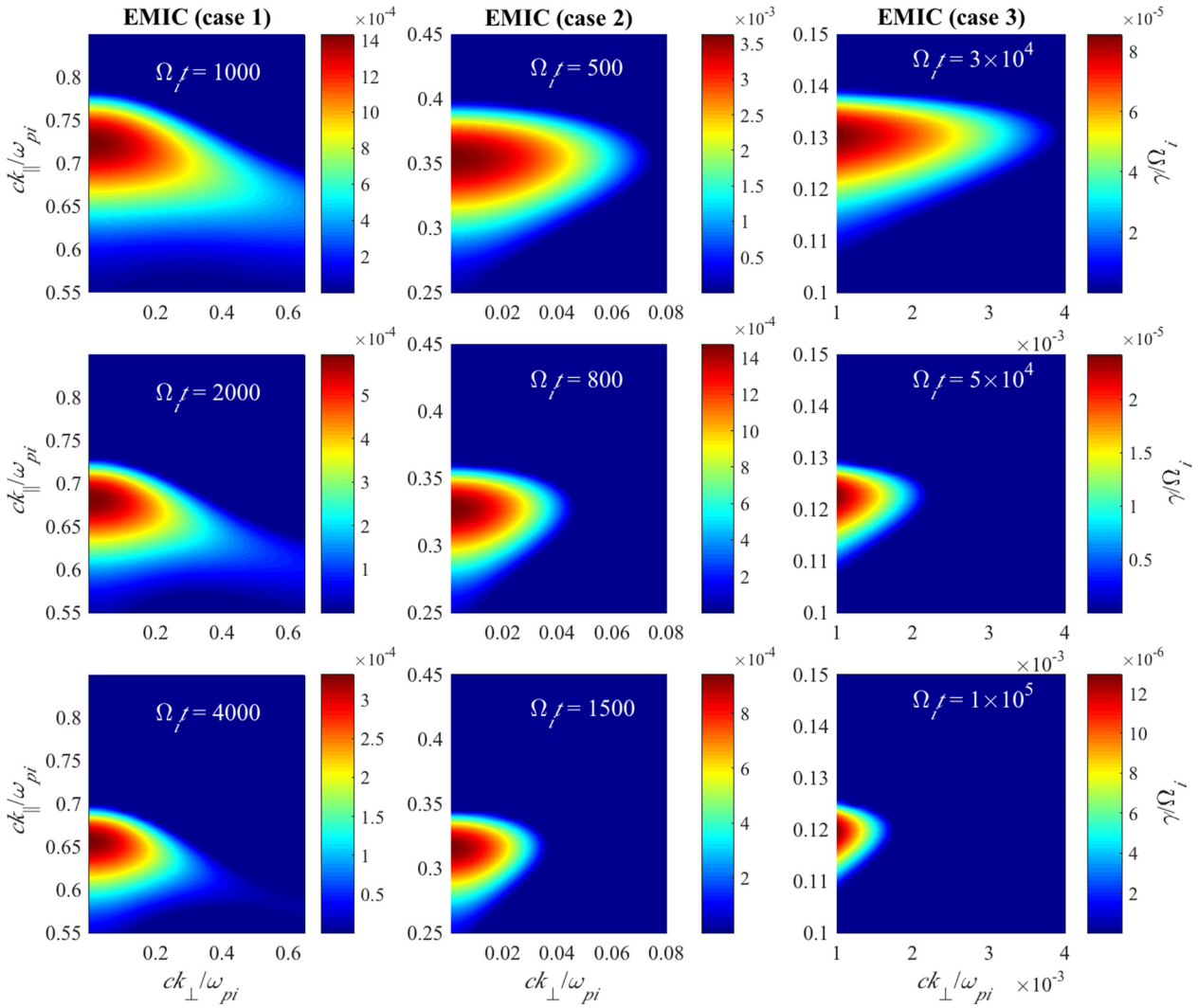

FIG. 6. The snapshots of instantaneous growth rate $\gamma_{\mathbf{k}}/\Omega_i$ for the three sample cases shown in Fig. 5, each at different time intervals. Note that for case 3, the x axis is defined over a very small perpendicular wave number range, $10^{-3} < ck_\perp/\omega_{pi} < 4 \times 10^{-3}$, which is indicated in the axis labels with an overall multiplicative factor $\times 10^{-3}$.

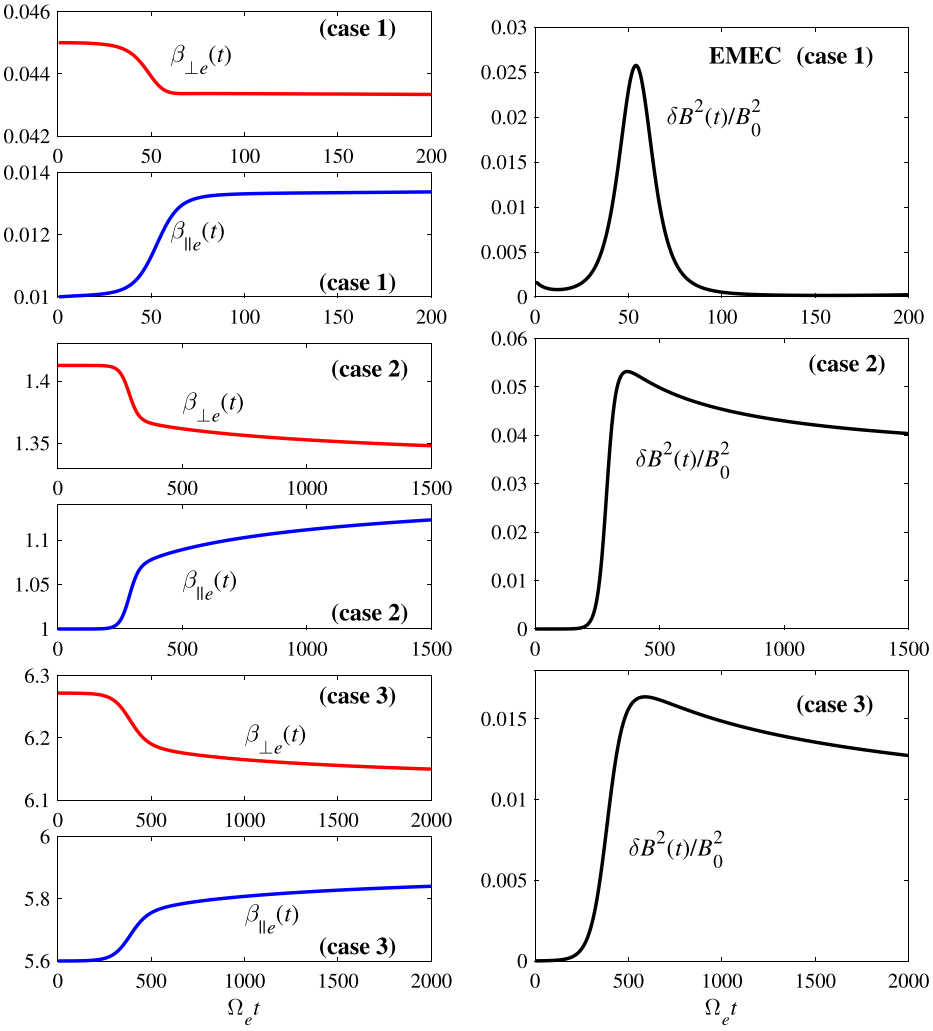

FIG. 7. Time evolution of the perpendicular and parallel betas, $\beta_{\perp e}(t)$ and $\beta_{\|e}(t)$ [left-hand panels] and normalized wave magnetic field energy density $\delta B^2(t)/B_0^2$ associated with EMEC instability [right] *versus* normalized time Ω_{et}. For the initial conditions, we chose $\beta_{\|e}(0) = 0.1$ and $T_{\perp e}(0)/T_{\|e}(0) = 4.5$ (case 1), $\beta_{\|e}(0) = 1$ and $T_{\perp e}(0)/T_{\|e}(0) = 1.14125$ (case 2), and $\beta_{\|e}(0) = 5.6$ and $T_{\perp e}(0)/T_{\|e}(0) = 1.12$ (case 3).

indicated in Fig. 2, namely, $\beta_{\|e}(0) = 0.1$ and $T_{\perp e}(0)/T_{\|e}(0) = 4.5$ (case 1), $\beta_{\|e}(0) = 1$ and $T_{\perp e}(0)/T_{\|e}(0) = 1.14125$ (case 2) and $\beta_{\|e}(0) = 5.6$ and $T_{\perp e}(0)/T_{\|e}(0) = 1.12$ (case 3). The middle panel plots $\beta_{\|e}(t)$ *versus* normalized time Ω_{et} and the bottom panel plots the normalized wave magnetic field energy density associated with EMEC instability

$$\frac{\delta B^2(t)}{B_0^2} = \int d\mathbf{k}\, \frac{c^2 k^2}{\omega_{\mathbf{k}}^2} \frac{\langle \delta E_{\mathbf{k}}^2 \rangle}{B_0^2}, \tag{35}$$

versus Ω_{et}. For all three cases, the initial electron temperature anisotropy corresponds to $T_{\perp e}(0)/T_{\|e}(0) = 4$. As EMIC instability is excited, the temperature ratio is reduced while the electrons are heated in the parallel direction. Among the three cases, case 1 with high initial parallel beta implies the highest initial growth rate. As such, the wave growth shown in the bottom panel is the fastest for case 1, followed by cases 2 and 3. The anisotropy reduction and parallel heating are also in accordance with the magnitude of initial parallel electron beta. Again, in all the cases we have checked the conservation of the total energy (33), and indeed, the energy conservation is preserved.

As discussed by Refs. 3 and 4, EMEC instability for low β is characterized by the maximum growth rate occurring for the oblique wave propagation angle. Figure 8 plots the instantaneous growth rate, $\gamma_{\mathbf{k}}/\Omega_e$, for the three cases. The left-hand panels, which correspond to case 1 parameters show that indeed, the EMEC instability is highly oblique. As the instability progresses, the instantaneous growth rate is generally reduced in magnitude and the range of unstable modes shrinks.

V. SUMMARY

Kinetic plasma instabilities are important for regulating the temperature anisotropies in solar wind,[8–13] and they are one of the outstanding problems in the contemporary space and astrophysics to model large scale or macroscopic solar wind quantities by incorporating kinetic/microscopic physics into the global model of the solar wind.[14–18] In such efforts, one must generally allow various instabilities to operate simultaneously and compete for the available free energy, which resides with the temperature anisotropies. In this context, electromagnetic ion/electron cyclotron (EMIC/EMEC) instabilities, which are customarily discussed under the assumption of parallel propagation, must be extended to two- or three-dimensional configurations, since other instabilities such as mirror and oblique fire hose instabilities are operative for general propagation directions. The aim of the present paper was to develop analytical models of 2 D EMIC and EMEC instabilities within the context of linear and quasilinear formalisms so that eventually the theoretical

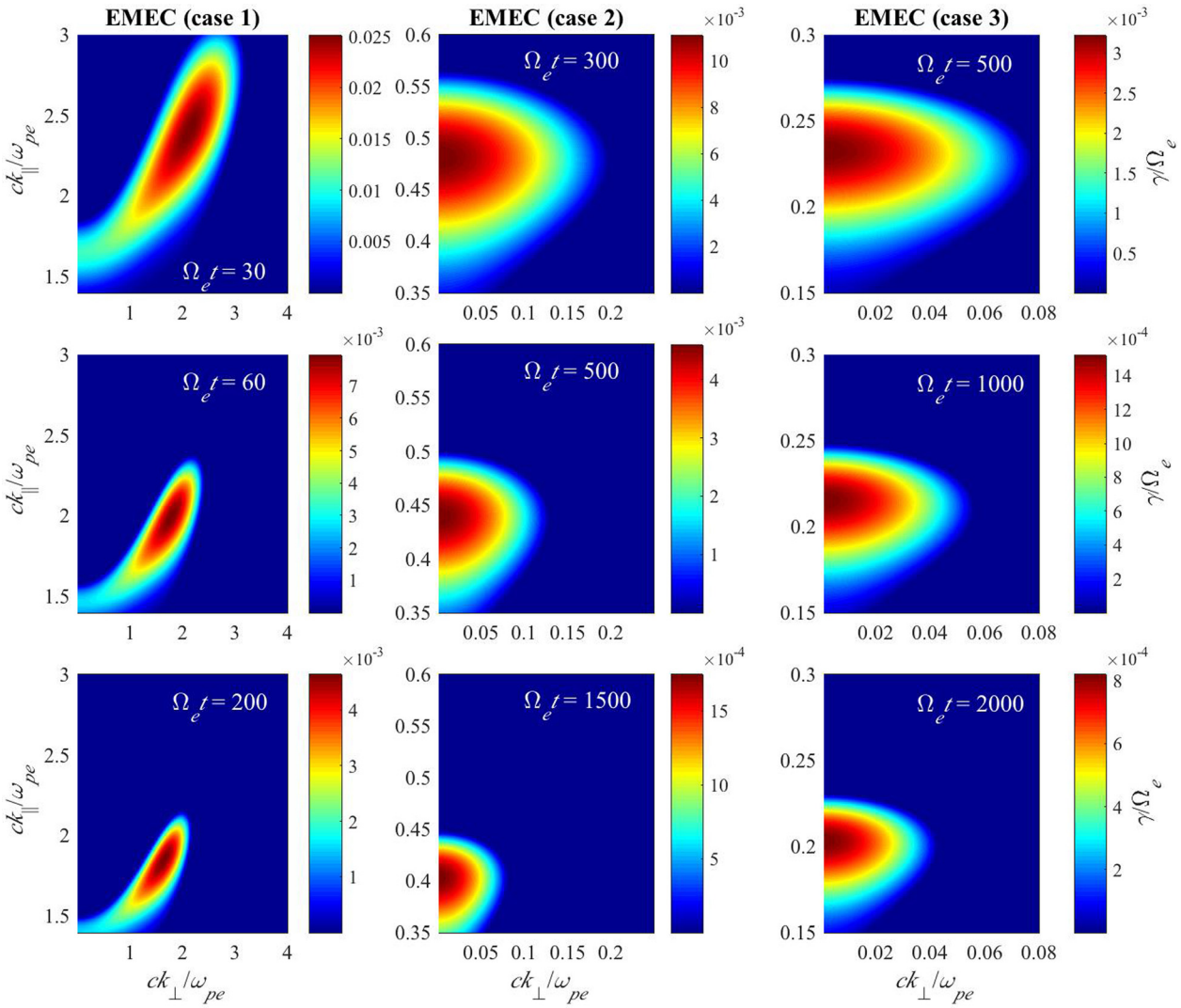

FIG. 8. The instantaneous growth rate $\gamma_{\mathbf{k}}/\Omega_e$ for three cases is plotted *versus* $ck_\perp/\omega_{pe}$ and $ck_\parallel/\omega_{pe}$.

formalism developed in the present paper may be generalized to include other unstable modes.

Our aim had been to limit the scope of the theoretical development to the weakly growing instability regime. For such a situation, it is generally acceptable to treat the real frequency with the cold plasma approximation while computing the growth rate with the approximate Landau type of formula. For a high instability growth rate, which is not the focus of the present paper, the problem generally requires the full solution of the transcendental dispersion relation that involves the plasma dispersion function with complex frequency. Such a task is beyond the scope of the present discussion, and some preliminary work along this line can be found in the literature.[19]

To summarize the major findings and to recapitulate the present investigation, in Sec. II we first validated the approximate approach by comparing against the exact solutions, based upon which we chose three representative input parameters for both EMIC and EMEC instabilities, which were extrapolated for the general case of arbitrary propagation. We then formulated the analytical model of the linear theory of 2 D EMIC and 2 D EMEC instabilities. In Sec. III, we extended the analysis to the quasilinear regime. In order to simplify the quasilinear analysis, we assumed that the particle velocity distribution functions maintain the bi-Maxwellian form, which is an approximation, but previous comparative studies by Refs. 25–27, and to a certain extent, the simulation by Ref. 4, showed that such an assumption is valid at least as a first cut approach. In the subsequent Sec. IV, we presented some sample numerical results in order to demonstrate the outcome of the present theoretical formalism.

In the future, we plan to make use of the present formalism to explore the quasilinear development of these instabilities as they compete with other unstable modes such as the electron/proton mirror instability.[7] Such a calculation may be useful in understanding the recent simulation work by Ahmadi *et al.*[5] or by Riquelme *et al.*,[6] for instance. Finally, the present analytical approach may be applied to the situation beyond the strict bi-Maxwellian models. One of the limitations of relying on exact linear Vlasov analysis is that the computation of the velocity integral is severely constrained by the choice of particle velocity distributions. However, for a relatively weak instability growth rate, for which the

present analytical method is applicable, it may be possible to analyze the unstable properties of the plasma without being restricted by the mathematical choice of the underlying particle velocity distribution function.

ACKNOWLEDGMENTS

N.N. acknowledges support from the Higher Education Commission (HEC), Pakistan. P.H.Y. acknowledges NSF Grant No. AGS1550566 to the University of Maryland and the BK21 plus program from the National Research Foundation (NRF), Korea, to the Kyung Hee University.

[1]S. P. Gary and H. Karimabadi, J. Geophys. Res. **111**, A11224, https://doi.org/10.1029/2006JA011764 (2006).
[2]S. P. Gary, M. D. Montgomery, W. C. Feldman, and D. W. Forslund, J. Geophys. Res. **81**, 1241, https://doi.org/10.1029/JA081i007p01241 (1976).
[3]S. P. Gary and I. H. Cairns, J. Geophys. Res. **104**, 19835, https://doi.org/10.1029/1999JA900296 (1999).
[4]S. P. Gary, K. Liu, and D. Winske, Phys. Plasmas **18**, 082902 (2011).
[5]N. Ahmadi, K. Germaschewski, and J. Raeder, J. Geophys. Res. **121**, 5350, https://doi.org/10.1002/2016JA022429 (2016).
[6]M. A. Riquelme, E. Quataert, and D. Verscharen, Astrophys. J. **824**, 123 (2016).
[7]N. Noreen, P. H. Yoon, R. A. López, and S. Zaheer, J. Geophys. Res. **122**, 6978, https://doi.org/10.1002/2017JA024248 (2017).
[8]S. P. Gary and J. Wang, J. Geophys. Res. **101**, 10749, https://doi.org/10.1029/96JA00323 (1996).
[9]P. Hellinger, P. Trávníček, J. C. Kasper, and A. J. Lazarus, Geophys. Res. Lett. **33**, L09101, https://doi.org/10.1029/2006GL025925 (2006).
[10]Š. Štverák, P. Trávníček, M. Maksimovic, E. Marsch, A. N. Fazakerley, and E. E. Scime, J. Geophys. Res. **113**, A03103, https://doi.org/10.1029/2007JA012733 (2008).
[11]P. Hellinger and P. Trávníček, Astrophys. J. Lett. **784**, L15 (2014).
[12]M. Lazar, S. Poedts, R. Schlickeiser, and C. Dumitrache, Mon. Not. R. Astron. Soc. **446**, 3022 (2015).
[13]M. L. Adrian, A. F. Viñas, P. S. Moya, and D. E. Wendel, Astrophys. J. **833**, 49 (2016).
[14]B. D. G. Chandran, T. J. Dennis, E. Quataert, and S. D. Bale, Astrophys. J. **743**, 197 (2011).
[15]D. Verscharen, B. D. G. Chandran, K. G. Klein, and E. Quataert, Astrophys. J. **831**, 128 (2016).
[16]P. H. Yoon and M. Sarfraz, Astrophys. J. **835**, 246 (2017).
[17]S. M. Shaaban, M. Lazar, S. Poedts, and A. Elhanbaly, Astrophys. Space Sci. **362**, 13 (2017).
[18]P. Hunana and G. Zank, Astrophys. J. **839**, 13 (2017).
[19]P. H. Yoon and J. Seough, J. Geophys. Res. **117**, A08102, https://doi.org/10.1029/2012JA017697 (2012).
[20]S. P. Gary, *Theory of Space Plasma Microinstabilities* (Cambridge University Press, Cambridge, 2005).
[21]J. Seough and P. H. Yoon, J. Geophys. Res. **117**, A08101, https://doi.org/10.1029/2012JA017645 (2012).
[22]D. Verscharen, S. Bourouaine, B. D. G. Chandran, and B. Maruca, Astrophys. J. **773**, 8 (2013).
[23]D. B. Melrose, *Plasma Astrophysics* (Gordon and Breach, New York, 1980).
[24]C. F. Kennel and F. Engelmann, Phys. Fluids **9**, 2377 (1966).
[25]J. Seough, P. H. Yoon, and J. Hwang, Phys. Plasmas **21**, 062118 (2014).
[26]M. Lazar, P. H. Yoon, and B. Eliasson, Phys. Plasmas **24**, 042110 (2017).
[27]H. P. Kim, J. Hwang, J. J. Seough, and P. H. Yoon, J. Geophys. Res. **122**, 4410, https://doi.org/10.1002/2016JA023558 (2017).